

## Numerical study on heat and flow transfer of biomagnetic fluid with copper nanoparticles over a linear extended sheet under the influence of magnetic dipole and thermal radiation


Mohammad Ghulam Murtaza<sup>1</sup>, Maria Akter<sup>1</sup> and Mohammad Ferdows<sup>2\*</sup>

<sup>1</sup> Department of Mathematics, Comilla University, Cumilla, **BANGLADESH**

<sup>2</sup> Research Group of Fluid Flow Modeling and Simulation, Department of Applied Mathematics, University of Dhaka, Dhaka, **BANGLADESH**

\* Corresponding Author: [ferdows@du.ac.bd](mailto:ferdows@du.ac.bd)

Received Oct 28<sup>th</sup> 2023; Revised Dec 04<sup>th</sup> 2023; Accepted Dec 06<sup>th</sup> 2023

 Cite this <https://doi.org/10.24036/teknomekanik.v6i2.26972>

**Abstract:** A steady, two-dimensional flow of biomagnetic fluid namely blood flow with copper nanoparticles across a stretchable sheet that is affected by a strong magnetic field and thermal radiation is investigated in this study. Copper nanoparticles (Cu-NPs) were used for this study because of their important applicability in biomedical research. Thus, the properties of copper nanoparticles render it an antibacterial, antimicrobial, and anti-fungal material. Similarity substitutions were applied to reduce the nonlinear partial differential equations to ordinary differential equations. Utilizing the MATLAB R2018b software `bvp4c` function technique, the physical solution was established. This model's pertinent dimensions, such as the ferromagnetic parameter, the magnetic field parameter, the radiation parameter, the suction parameter, the ratio parameter, the slip parameter, and the Prandtl Number, were computationally and graphically inspected about the dimensionless velocity, temperature, skin friction, and heat transfer rate. One of the pivotal observations was that a rise in the ferromagnetic parameter and Prandtl number drops the temperature and velocity, correspondingly. A cross-case analysis with the outcome of other published research is also executed for divergent parameter values. Based on the investigations, copper nanoparticles may be advantageous for biomedical purposes and lessen the hemodynamics of stenosis. Owing to the research, copper nanoparticle-concentrated blood exhibits a reduced flow impedance and a larger temperature changeability compared to sheer blood.

**Keywords:** Biomagnetic Fluid Dynamics; Copper Nanoparticles; Blood; Magnetic Dipole

### 1. Introduction

Understanding, modulating, assessing, or mending human organs and tissues using internal or external magnetic fields is the purpose of the interdisciplinary field of biomagnetic fluid dynamics. Biomagnetic fluid uses have evolved to involve diagnosing neurological or cardiac disorders as well as comprehending the underlying mechanics of the human brain and heart throughout the last several decades. Researchers in the realms of biomedical engineering and its linked sciences have spurred the introduction of innovative biotechnologies. The fluid flow is analyzed using ferrohydrodynamic (FHD) and magneto-hydrodynamic (MHD) principles, and the magnetic field is adequately covered by a computational grid, in the current model.

The broad modern utilizations of the investigation of limit layer conduct overextending sheet issues, for example, the streamlined expulsion of plastic sheets, the displacement of a polymer sheet from colour, the buildup cycle of metallic plates in cooling showers, and some designing applications, like the development of paper, metal turning, the production of food sources, the streamlined expulsion of plastic and elastic sheets, and so on, have drawn attention to the research. Mansur et al.[1] have been utilizing the Buongiorno model to investigate the progression of stagnation

highlighting a porous sheet of extending/contracting with the impact of pull in a nanofluid. They observed that the skin friction decreases as the sheet is extended, but rises as the impact of suction increases. Jat et al. [2], [3] studied the MHD flow of the boundary layer past the stagnation point of an extending linear surface. Wang [4] studied the stagnation point flow caused by a linearly shrinking surface. Aman et al. [5] observed the continuous flow of a two-dimensional stagnation point in a viscous fluid within the magnetic field through a linear sheet of stretching and shrinking. The findings indicate that there are two distinct options for shrink wrap and stretch wrap. The concept of fluid flow over a stretching boundary layer was also investigated by Crane [6]. The fluid behaviour of viscous flow through a shrinking sheet was examined by Miklavčič et al. [7]. The impact of thermal radiation on blood flow subject to magnetic dipole over an extended sheet was discussed by Alam et al. [8]. Mahapatra and Gupta [9], [10] addressed the thermal performance in the flow of a stagnation point across a sheet stretched over a viscoelastic fluid.

Vajravelu, on the other hand, was the first researcher to examine the flow of viscous fluid past a nonlinear stretching sheet [11]. It was discovered that the fluid has consistently received heat flow from the stretching sheet. Similarity solutions for the stagnation point flow were examined by Bachok and Ishak [12] past a nonlinear sheet of stretching and shrinking. A well-known shooting method was used to solve the problem computationally. The behaviour of nanofluid flow caused by extendable non-linear sheets was further investigated by Rana et al. [13] Matin et al. [14] investigated what MHD meant for the drift of joined convective in a nanofluid past an extending sheet along entropy heat generation. A mathematical analysis of electrically conducting fluid over a stretchable boundary layer through a porous medium under chemical reaction and transverse magnetic field was discussed by Cortell [15]. Moreover, in [16] Cortell discussed the behaviour of viscous fluid flow under two surface temperature conditions. One is constant surface temperature and the other one is prescribed surface temperature. Raptis et al. [17] investigated thick drift over a nonlinear stretching sheet in the presence of a chemical response and a magnetic field. Tzirtzilakis first discussed the mathematical model of biomagnetic fluid which is based on Haik et al. in [18]. The extended mathematical model of BFD using MHD and FHD principles through a stretchable cylinder was discussed by Alam et al. [19] and shows that blood flow has a significant influence on the boundary layer compared to conventional blood flow. Recently a respectable study of boundary layer flow under several circumstances has been conducted by [20], [21], [22].

Due to the staggering number of potential applications in the fields of biomedicine, and bioengineering, nanoparticle evaluation has quickly become a hotbed of intense research interest. The terminology "nanofluid" implies a composition of a substrate liquid and nanoparticles having distinctive chemical and bodily attributes. Non-metals like nitrides and metals like carbon nanotubes and graphite contain the majority of the nanoparticles. Manufacturing, computers, microelectronics, transportation, biomedicine, food processing, fuel cells, solid-state lighting, and the heat transfer rates of microchips are just a few examples of their applications.

Choi was the first person to use the word "nanofluid"[23]. Recently, the heat and flow characteristics of blood flow containing magnetic particles past a stretchable cylinder under the magnetic dipole effect were described by Ferdows et al. [24]. Ferdows et al. [25] discussed the blood behaviour in three cases namely FHD, MHD and extension of MHD and FHD i.e. BFD. They observed that blood temperature was the highest found in the case of BFD compared to MHD and FHD, where ferromagnetic numbers play a key role over the flow boundary layer. A comprehensive comparison of magnetic and non-magnetic particles when injected into blood flow was found [26]. Using Newtonian heating, Hayat et al. [27] examined homogeneous-heterogeneous reactions in the stagnation point flow of carbon nanotubes. Utilizing Ti and Ti-alloy nanoparticles on blood (as the base fluid), Reddy et al. [28] found the importance of nanofluid across a non-linear stretching sheet with the velocity slip.

However, the aforementioned, studies reveal that the study of biomagnetic fluid containing nanoparticles over an extendable sheet using the ferrohydrodynamics concept has not yet been studied to date with the author's best knowledge. Blood is considered a base fluid which is electrically non-conducting and has properties of magnetization. Additionally, the impacts of velocity slip and thermal radiation are also considered. The addressed govern flow problem is expressed in PDEs form which is converted into ODEs with the help of suitable similarity transformations. A bvp4c technique is then used to show the physical insight of governing dimensionless parameters.

## 2. Material dan methods

### 2.1 Mathematical formulation

Assuming a laminar flow of blood-Cu in two dimensions through a stretching/shrinking sheet controlled by velocity slip. The non-linear velocity for the stretching/shrinking sheet is  $u_w(x) = cx^m$ , and the power index is represented by "m" and indicates stretching when  $c > 0$  and shrinking sheet  $c < 0$ , respectively. The surface temperature is assumed  $T_w$  and the ambient temperature far away from the sheet is  $T_\infty$  such that  $T_w < T_\infty$ . It is also assumed that for being applied to a magnetic field, a magnetic dipole is produced at distance d from the sheet. Additionally, consider that the y-axis is taken perpendicular to the sheet whereas the x-axis is taken along.

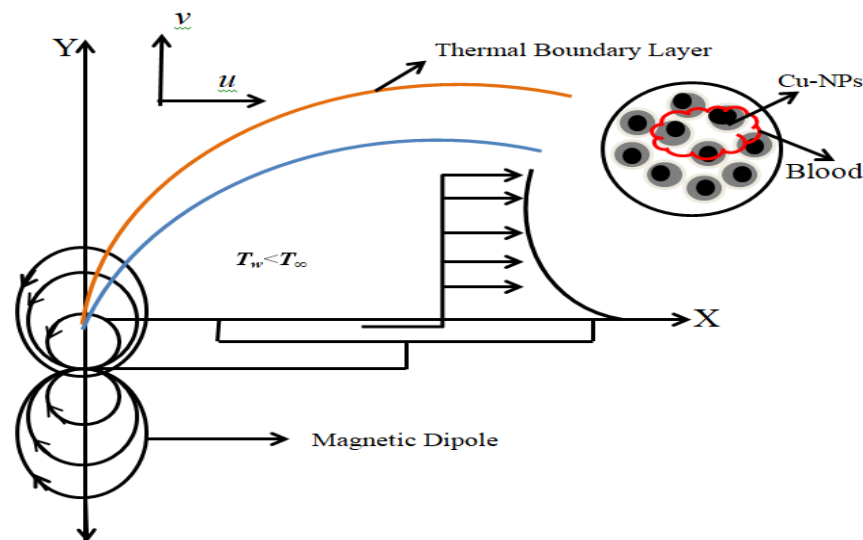


Figure 1: Sketch of physical problem

From the above assumption, the governing boundary layer equations of the flow are given as follows by [24], [25], [29].

$$u \frac{\partial u}{\partial x} + v \frac{\partial v}{\partial y} = 0 \tag{1}$$

$$u \frac{\partial u}{\partial x} + v \frac{\partial v}{\partial y} = u_e \frac{\partial u_e}{\partial x} + \frac{\mu_{nf}}{\rho_{nf}} \left( \frac{\partial^2 u}{\partial y^2} \right) + \frac{1}{\rho_{nf}} \mu_0 M \frac{\partial H}{\partial x} \tag{2}$$

$$u \frac{\partial T}{\partial x} + v \frac{\partial T}{\partial y} + \frac{\mu_0}{(\rho C p)_{nf}} T \frac{\partial M}{\partial T} \left( u \frac{\partial H}{\partial x} + v \frac{\partial H}{\partial y} \right) = \alpha_{nf} \left( \frac{\partial^2 T}{\partial y^2} \right) + \frac{1}{(\rho C p)_{nf}} \left( \frac{\partial q_r}{\partial y} \right) \tag{3}$$

With boundary conditions:

$$u = cx^m + U_{slip}, v = v_w, T = T_w = T_\infty + c_1 x^n \tag{4}$$

$$u = u_e = c_\infty x^m, T \rightarrow T_\infty, \text{ at } y \rightarrow \infty \tag{5}$$

Here,  $u$  and  $v$  denoted the components of velocity along (*the x, and y*) directions, respectively. Also,  $u_e$  is the free stream velocity,  $\mu$  is the viscosity under dynamic conditions,  $\mu_{nf}$  is the effective friction coefficient in motion,  $\rho_{nf}$  is the effective density of the nanofluid,  $T$  is the nanofluid temperature,  $(\rho C_p)_{nf}$  is the thermal capacity of the base fluid,  $M$  is the magnetization of the fluid.

Thermophysical correlation of nanofluid model can be expressed by:

$$\mu_{nf} = \frac{\mu_{nf}}{(1-\phi)^{2.5}}, \alpha_{nf} = \frac{K_{nf}}{(\rho C_p)_{nf}}, \rho_{nf} = (1-\phi)\rho_f + \phi\rho_s, k_{nf} = k_f \left[ \frac{k_s + 2k_f - 2\phi(k_f - k_s)}{k_s + 2k_f + 2\phi(k_f + k_s)} \right], M = K(T_w - T) \tag{6}$$

Where ' $\phi$ ' signifies the volume fraction of nanoparticles,  $k_{nf}$  is the nanofluid's thermodynamic resistance  $\mu_f$ , is the viscosity under dynamic conditions,  $\rho_f$  and  $\rho_s$  are the densities of fluid and solid,  $k_f$  and  $k_s$  are thermal conductivities of fluid and solid, respectively. Velocity slip relations of governing boundary layer equations are considered by  $U_{slip} = A^* \frac{\partial u}{\partial y}$ .

The term  $\mu_0 M \frac{\partial H}{\partial x}$  in Eq. (2) denotes ferromagnetic body force per unit volume. In Eq. (3), the term  $\mu_0 T \frac{\partial M}{\partial T} \left( u \frac{\partial H}{\partial x} + v \frac{\partial H}{\partial y} \right)$  precedes the heating due to adiabatic magnetism. The vertical and horizontal electromagnetic field fluctuations are induced by,

$$\frac{\partial H}{\partial x} = \frac{\gamma}{2\pi} \left( \frac{-2x}{(y+d)^4} \right), \frac{\partial H}{\partial y} = \frac{\gamma}{2\pi} \left[ \frac{-2}{(y+d)^3} + \frac{4x^2}{(y+d)^5} \right] \tag{7}$$

Bodily force is inversely proportional to slope amplitude  $H$ , which yields

$$H(x, y) = [H_{x^2} + H_{y^2}]^{\frac{1}{2}} = \frac{\gamma}{2\pi} \left[ \frac{1}{(y+d)^2} - \frac{x^2}{(y+d)^4} \right] \tag{8}$$

The influence of magnetization  $M$  on temperature  $T$  is stated as  $M = K(T_w - T)$  where  $K$  is the pyromagnetic coefficient.

## 2.2 Dimensionless analysis

To make the governing equation dimensionless, the following variables are introduced.

$$\eta = \left( \frac{(m+1)u_w(x)}{2\nu_f x} \right)^{\frac{1}{2}} y, \psi = \left( \frac{2\nu_f x u_w(x)}{m+1} \right)^{\frac{1}{2}} f(\eta), \theta(\eta) = \frac{T - T_\infty}{T_w - T_\infty} \tag{9}$$

The continuity equation will be satisfied by defining the stream function as,

$$u = \frac{\partial \psi}{\partial y}, v = -\frac{\partial \psi}{\partial x} \tag{10}$$

By introducing Eq. (10) to (5), the following ordinary differential equations are obtained:

$$\frac{1}{(1-\phi)^{2.5}} f''' + \left\{ (1-\phi) + \phi \frac{\rho_s}{\rho_f} \right\} (ff'' - (f')^2 - A^2) - \frac{2\beta\theta}{(\eta+\alpha)^4} = 0 \tag{11}$$

$$\left( \frac{k_{nf}}{k_f} + Nr \right) \theta'' + \left[ (1-\phi) + \phi \frac{(\rho C_p)_s}{(\rho C_p)_f} \right] \text{Pr} (f\theta' - nf'\theta) - \frac{2\beta\lambda(\varepsilon+\theta)}{(\eta+\alpha)^3} f = 0 \tag{12}$$

The initial boundary conditions are:

$$f(0) = S, f'(0) = 1 + \lambda_1 f''(0), \theta(0) = 1, f'(\infty) = A, \theta(\infty) = 0 \tag{13}$$

Here,  $S = -v_w x^{-(m-1)/2} \sqrt{2/c(m+1)v_f}$  is defined as the suction/injection parameter ( $S > 0$  precedes the suction and  $S < 0$  precedes the injection respectively),  $\lambda_1 > 0$  represents first order velocity slip,  $A$  is the ratio of free stream velocity  $c_\infty$  to stretching velocity  $c$ .

Also, Prandtl number  $Pr = \frac{(\mu c_p)_f}{k_f}$ , viscous dissipation parameter  $\lambda = \frac{c \mu_f^2}{\rho_f k_f (T_c - T_w)}$ , dimensionless Curie temperature  $\varepsilon = \frac{T_\infty}{T_w - T_\infty}$ , dimensionless distance  $\alpha = \sqrt{\frac{c}{v_f}} d$ , radiation conduction parameter  $Nr = \frac{16\sigma^* T_\infty^3}{3k^* k_f}$ , ferromagnetic parameter  $\beta = \frac{\gamma}{2\pi} \frac{\mu_0 k (T_c - T_w) \rho_f}{\mu_f^2}$ .

In this research work, skin friction co-efficient  $C_f$  and local Nusselt number  $Nu$  are the quantities of practical interest and are defined as:

$$C_f = \frac{\tau_w}{\rho_f u_w^2} \tag{14}$$

$$Nu = \frac{x q_w}{k_f (T_w - T_\infty)} \tag{15}$$

The surface shearing stress  $\tau_w$  and the convective heat  $q_w$  are given by:

$$\tau_w = \mu_{nf} \left( \frac{\partial u}{\partial y} \right)_{y=0} \tag{16}$$

$$q_w = -k_{nf} \left( \frac{\partial T}{\partial y} \right)_{y=0} \tag{17}$$

Therefore, finally, we have the following form:

$$C_f Re^{\frac{1}{2}} = \frac{1}{(1-\phi)^{2.5}} f'''(0) \quad \& \quad Nu Re^{\frac{1}{2}} = -\frac{k_{nf}}{k_f} \theta'(0) \tag{18}$$

### 2.3 Numerical method for solution

For the solver (bvp4c) function in MATLAB software, the non-linear boundary value problem represented by Eq. (11) and (12) with the boundary condition Eq. (13) is solved consistently. To set the equations in MATLAB, new variables are added to Eq. (13) and (11) to make them first-order differential equations. The following are the brand-new initial variables:

$$f = y_1, f' = y_2, f'' = y_3, \theta = y_4, \theta' = y_5$$

Equations and boundary conditions undergo the following transformations into a system of first-order ordinary differential equations:

$$\begin{aligned} f' &= y_2, f'' = y_2' = y_3, \\ f''' = y_3' &= -(1-\phi)^{2.5} \left( 1 - \phi + \phi \frac{\rho_s}{\rho_f} \right) (y_1 y_3 - (y_2^2 - A^2)) + (1-\phi)^{2.5} \frac{2By_4}{(x+\alpha)^4} \end{aligned} \tag{19}$$



$$\theta'' = y_5' = \frac{1}{\left(\frac{k_{nf}}{k_f} + Nr\right)} \left[ - \left( 1 - \phi + \phi \frac{(\rho C p)_s}{(\rho C p)_f} \right) \text{Pr}(y_1 y_5 - n y_2 y_4) + \frac{2B\lambda(\varepsilon + \theta)}{(x + \alpha)^5} y_1 \right] \quad (20)$$

Under the following delimitation conditions:

$$y_1(0) = S, y_2(0) = 1 + \lambda_1 y_3(0), y_4(0) = 1, y_2(\infty) = A, y_4(\infty) = 0 \quad (21)$$

By a given proximate point, Eq. (19), (20) and (21) are compacted numerically as an initial value problem. The aforementioned simplifications are accomplished using the MATLAB software's bvp4c function.

### 3. Results and discussion

For numerical accuracy and validation of the present results, a comparison has been made with earlier studies of Mukhopadhyay [30] for several values of Prandtl number for  $NuRe^{\frac{1}{2}} = -\frac{k_{nf}}{k_f} \theta'(0)$  and this analysis is stated in Table 1.

Table 1: Value of  $NuRe^{\frac{1}{2}} = -\frac{k_{nf}}{k_f} \theta'(0)$  for several values of Prandtl number

| Pr | Mukhopadhyay | Present Study |
|----|--------------|---------------|
| 1  | 0.9547       | 0.9542        |
| 2  | 1.4714       | 1.4748        |
| 3  | 1.8961       | 1.8937        |

Since, in this model, blood is considered as base fluid and Cu as magnetic particles. So in the computational process, we utilize the following values that are captured in Table 2.

Table 2: Values of blood and Cu [31], [32]

| Properties                            | Base Fluid nano particles |      |
|---------------------------------------|---------------------------|------|
|                                       | Blood                     | Cu   |
| $C_p \left( jkg^{-1}K^{-1} \right)$   | $3.9 \times 10^3$         | 385  |
| $\rho \left( kgm^{-3} \right)$        | 1050                      | 8933 |
| $\kappa \left( Wm^{-1}K^{-1} \right)$ | 0.5                       | 400  |

However, the values of dimensionless parameters are that used in this model are for the numerical solution, specific values for the dimensionless parameters must be determined. In the case of fluid, like human blood, the body temperature is set at  $T_w = 37^\circ C = 310^0 K$  and the ambient temperature is  $T_\infty = 41^\circ C = 317^0 K$  [7]. For the given values, we have the following dimensionless parameters: the dimensionless temperature  $e = 78.5$  [33], Prandtl Number  $Pr = 21, 23, 25$  [19], radiation conduction parameter  $Nr = 0.2, 0.8, 1.0$ , viscous dissipation parameter  $\lambda = 0.01$ , ferromagnetic number  $B = 1, 5, 6$  [34], dimensionless distance  $\alpha = 0.5, 0.75, 1$  [34], volume friction  $\phi = 0.01, 0.05, 0.15$  [34], suction parameter  $S = 0.2, 0.5, 1.0$ , first order velocity slip parameter  $\lambda_1 = 0.1, 0.5, 1.0$ , ratio parameter  $A = 0.8, 0.9, 1.0$ , dimensionless Curie number  $\varepsilon = 78.5$  and linear stretching sheet  $n = 1$ . Unless otherwise noted in the relevant graphs, the values indicated above are conserved as common.

The temperature and velocity profiles for various ratio parameter values ( $A$ ) are shown in Figures 2 and 3. The figures show that both the velocity profile and temperature increase with increasing proportion thresholds in both the unadulterated blood and copper-adulterated blood cases. As the ratio parameter ( $A$ ) increases, the velocity and temperature profiles change as can be seen. The sheet and liquid both are moving at the same speed when  $A = 1.0$  is used. The non-dimensional flow function of the nano-fluid becomes increasingly positive between  $A = 0.8$  & and  $A = 0.9$ .

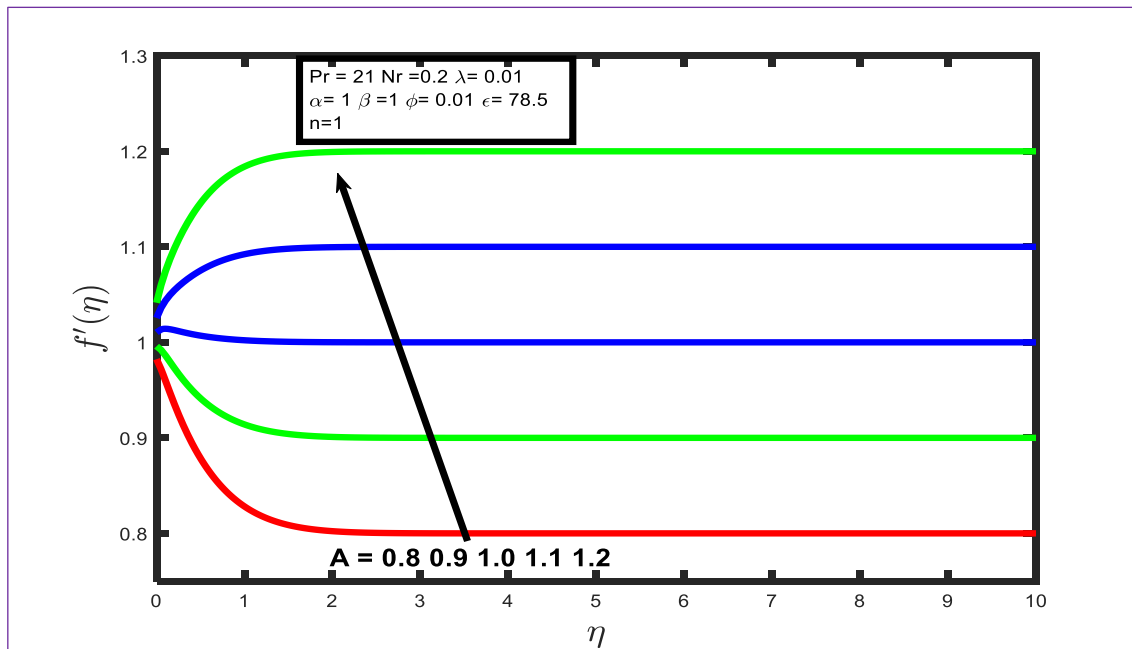


Figure 2: Effect of  $A$  on velocity profile  $f'(\eta)$

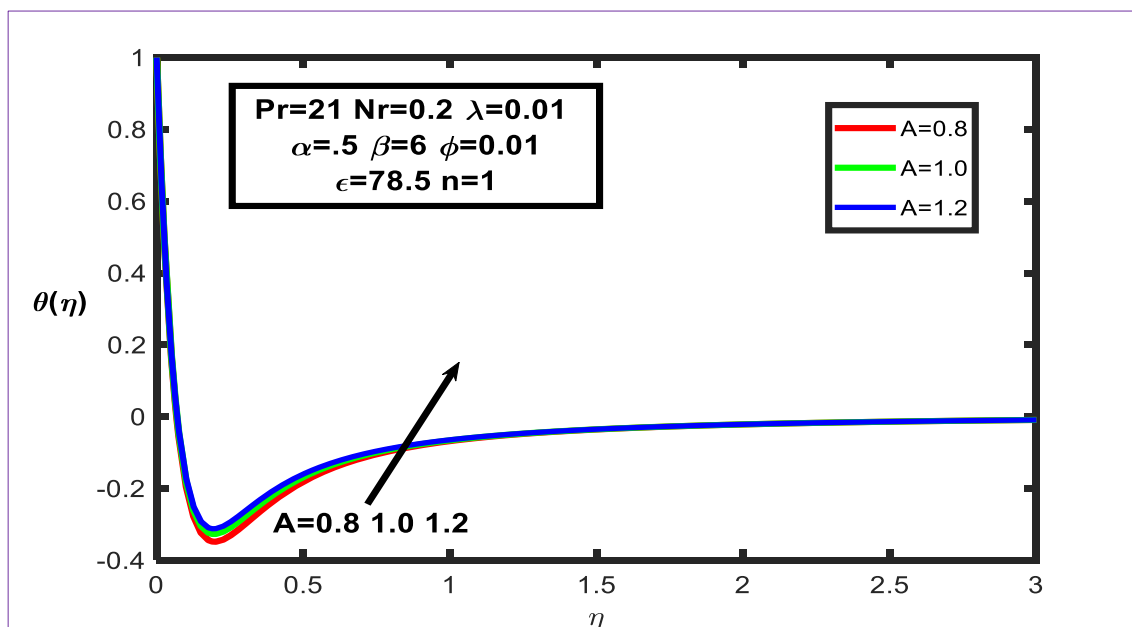


Figure 3: Effect of  $A$  on temperature profile  $\theta(\eta)$

The two figures 4 and 5 illustrate the velocity profile and heat flow for varying values of the non-dimensional range factor ( $\alpha$ ). The stats indicate that for two very different shear blood and copper shear blood, the velocity profile declines and the heat flow increases with increasing values of the non-dimensional range component.

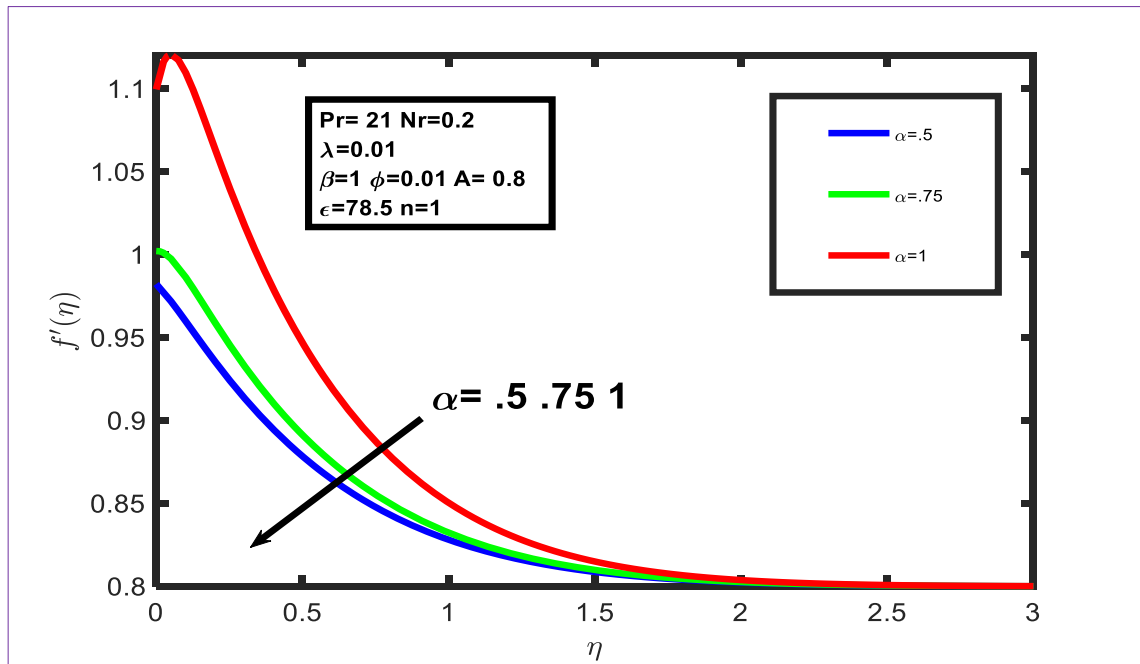


Figure 4: Effect of  $\alpha$  on velocity profile  $f'(\eta)$

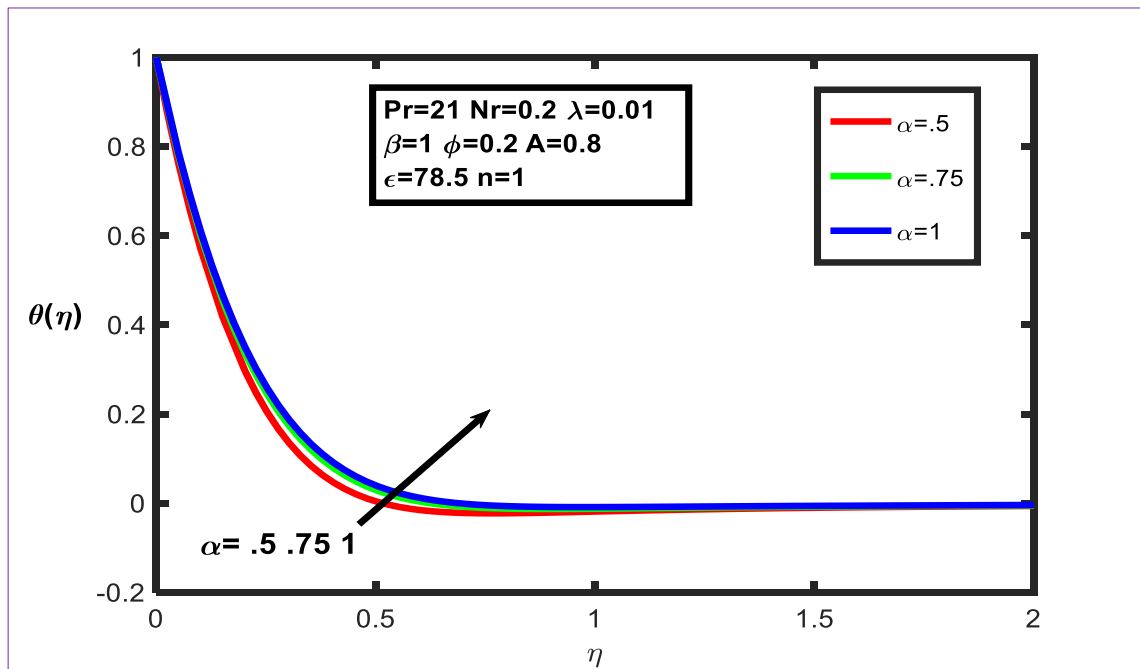


Figure 5: Effect of  $\alpha$  on temperature profile  $\theta(\eta)$

The influence of the speed profile and temperature profile for various upsides of ferromagnetic number ( $\beta$ ) is depicted in Figures 6 and 7. The graph demonstrates that the acceleration and temperature curve in copper sheer blood as well as sheer blood diminish as the ferrous quantity factors rise.



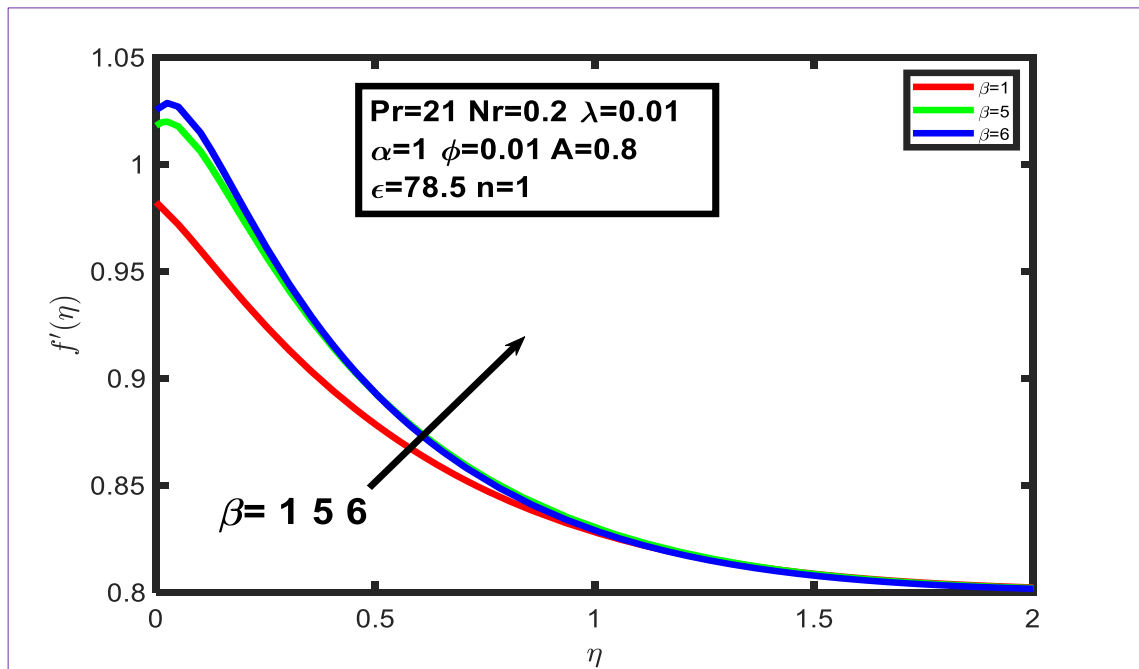


Figure 6: Effect of  $\beta$  on velocity profile  $f'(\eta)$

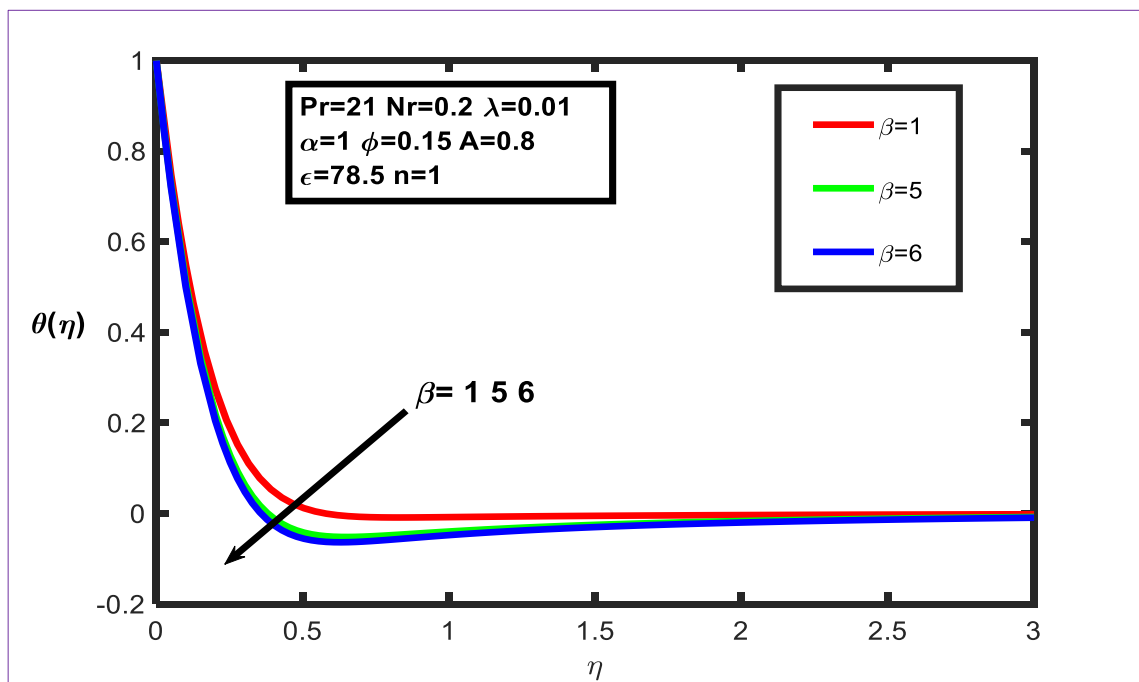


Figure 7: Effect of  $\beta$  on temperature profile  $\theta(\eta)$

Figures 8 and 9 illustrate the speed profile and heat flux considering multiple values of the first-order speed drop coefficient ( $\lambda_1$ ). As can be demonstrated from the figures, both pure blood and copper blood undergo temperature rises and a drop in the velocity profile with rising values for the slip effects at the fundamental level.

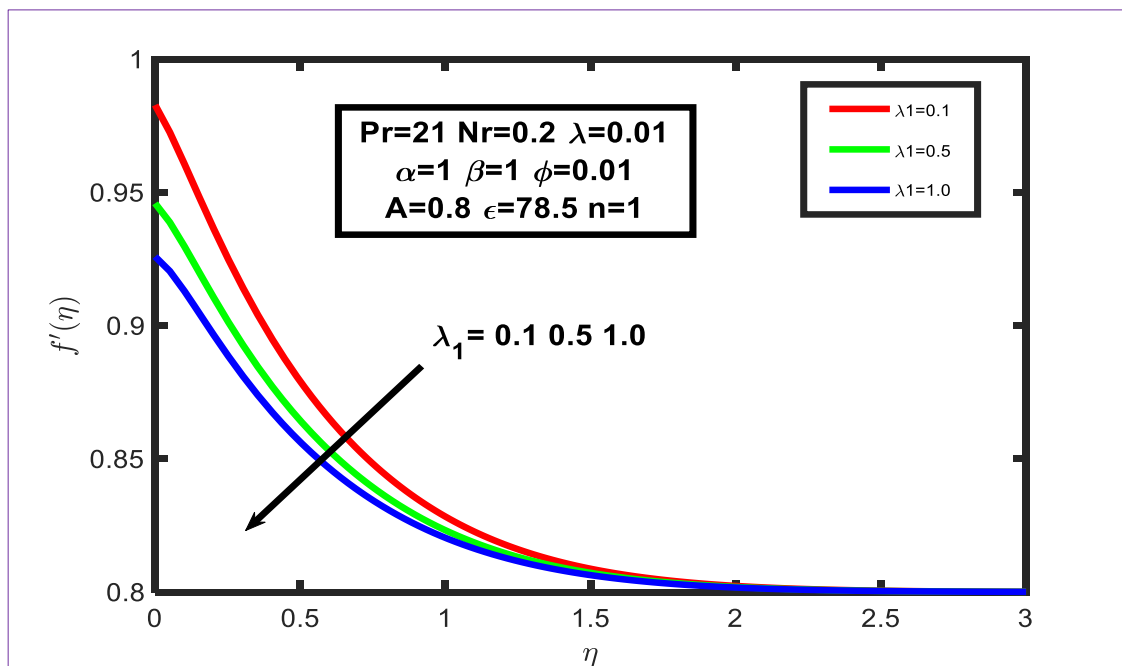


Figure 8: Effect of  $\lambda_1$  on velocity profile  $f'(\eta)$

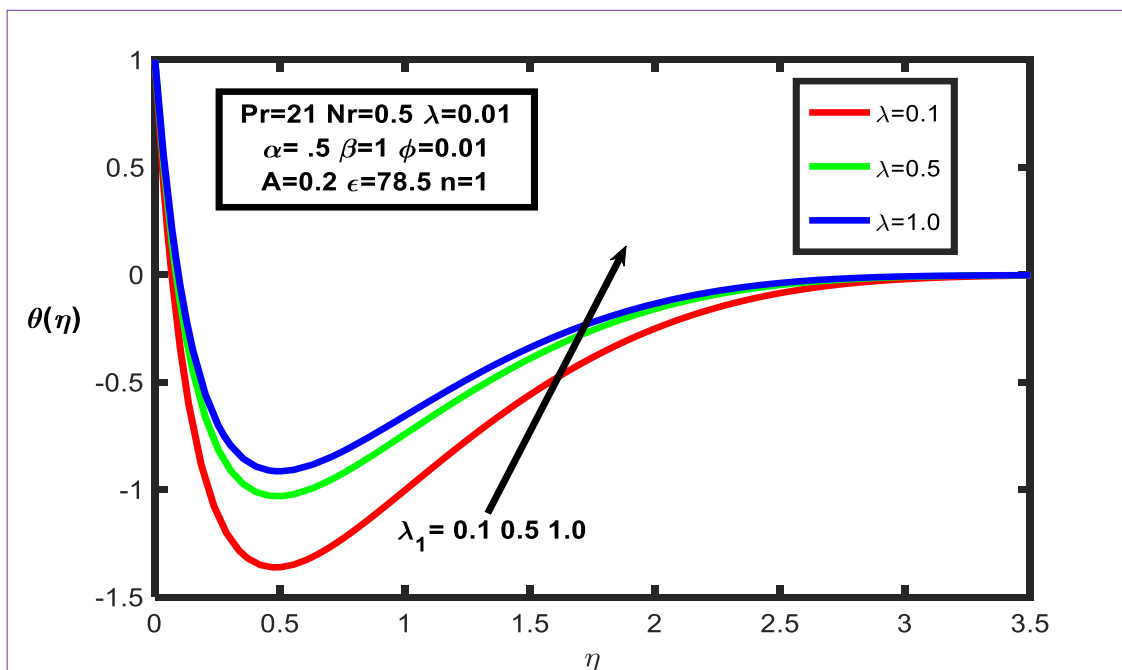


Figure 9: Effect of  $\lambda_1$  on temperature profile  $\theta(\eta)$

Demonstration of speed curve and heat flux profile for assorted values of radiation conduction constant ( $Nr$ ) are represented by Figures 10 and 11. As the radiation conductance factor is elevated in sheer blood and copper sheer blood, the speed curve and heat flux diminish.

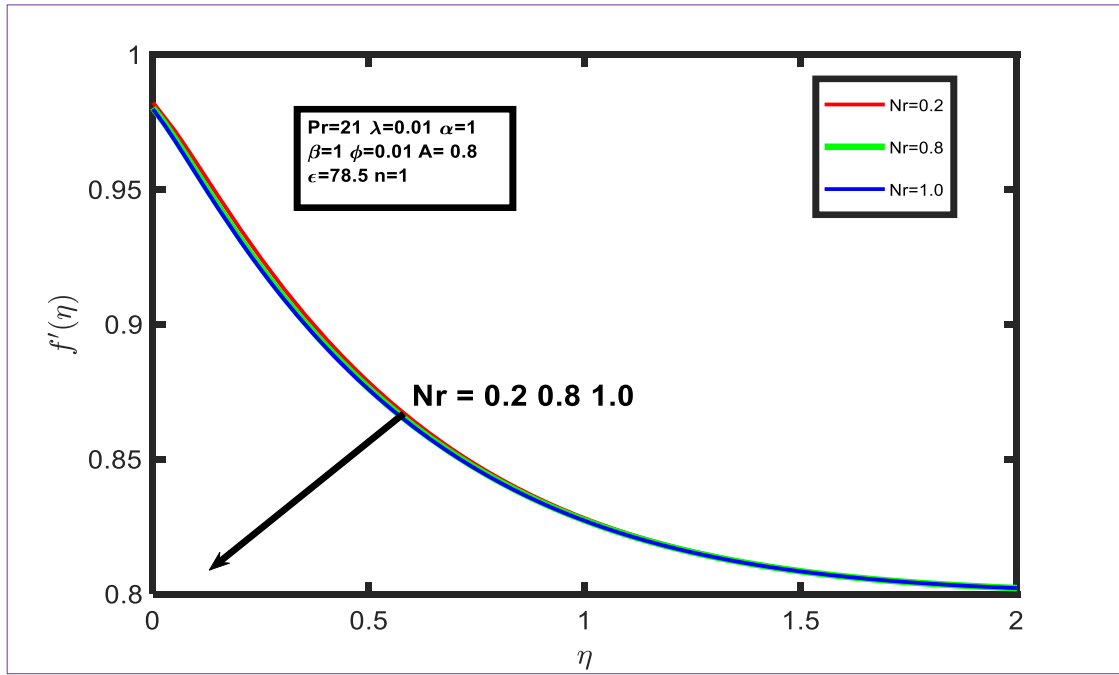


Figure 10: Effect of  $Nr$  on velocity profile  $f'(\eta)$

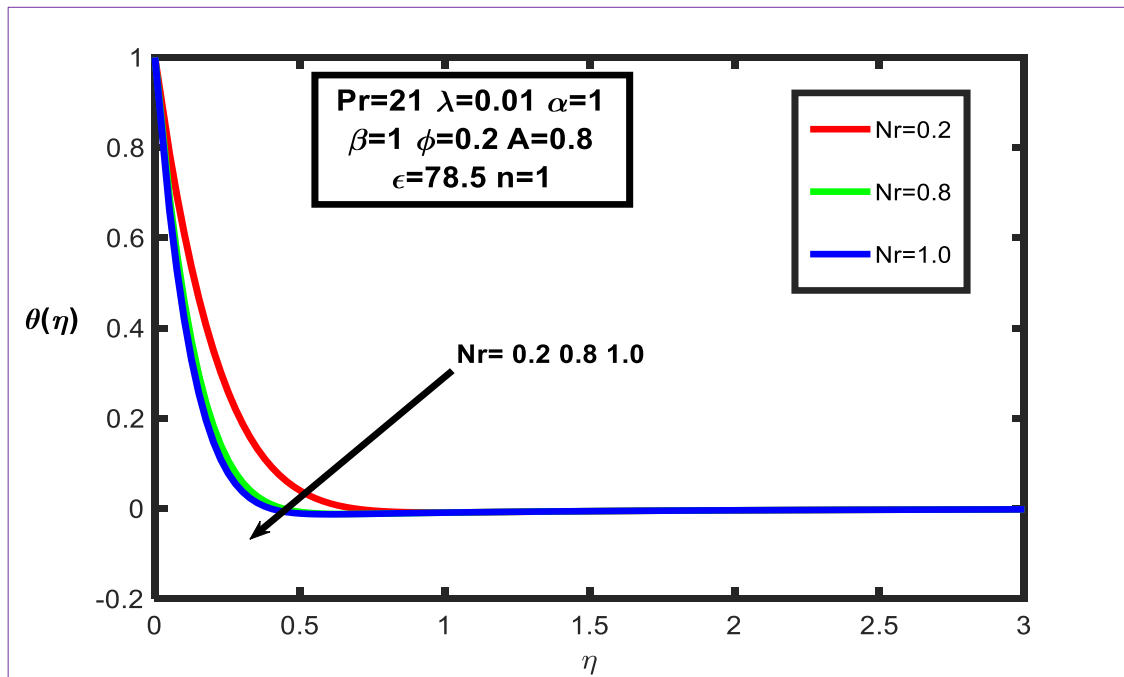


Figure 11: Effect of  $Nr$  on temperature profile  $\theta(\eta)$

Figures 12 and 13 illustrate the speed curve and heat flux for assorted values of the volume friction factor ( $\phi$ ). Analyzing the statistics, it tends to be apparent that the speed profile reduces and a surge in heat flux concomitant growing upsides of volume contact boundary in the two contexts for undiluted blood and copper undiluted blood.

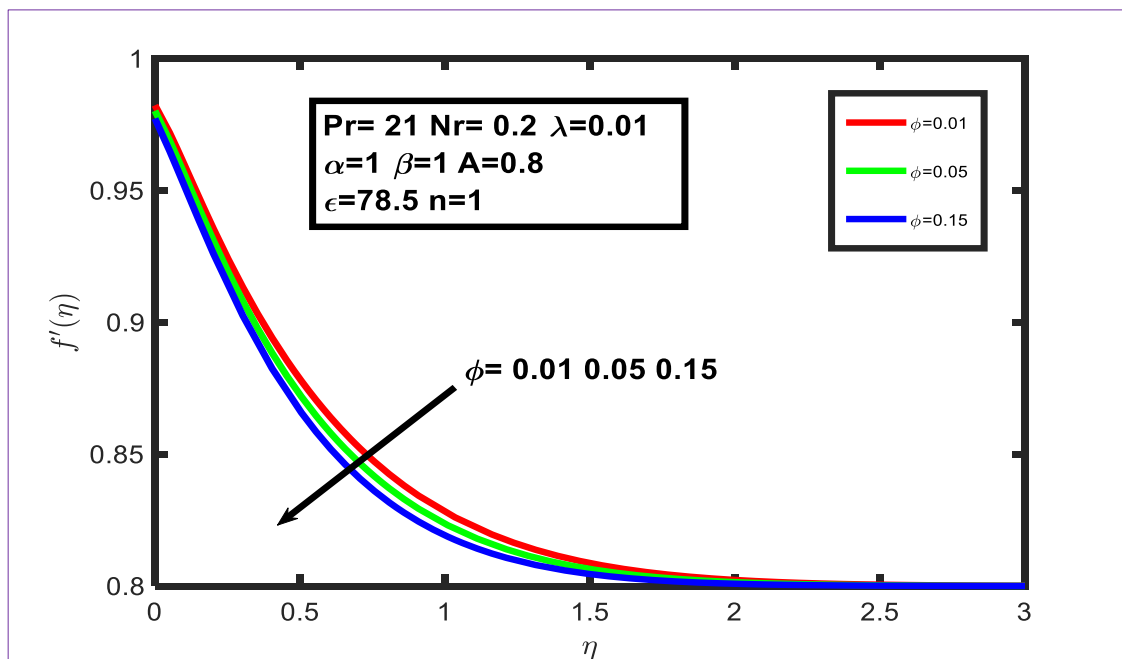


Figure 12: Effect of  $\phi$  on velocity profile  $f'(\eta)$

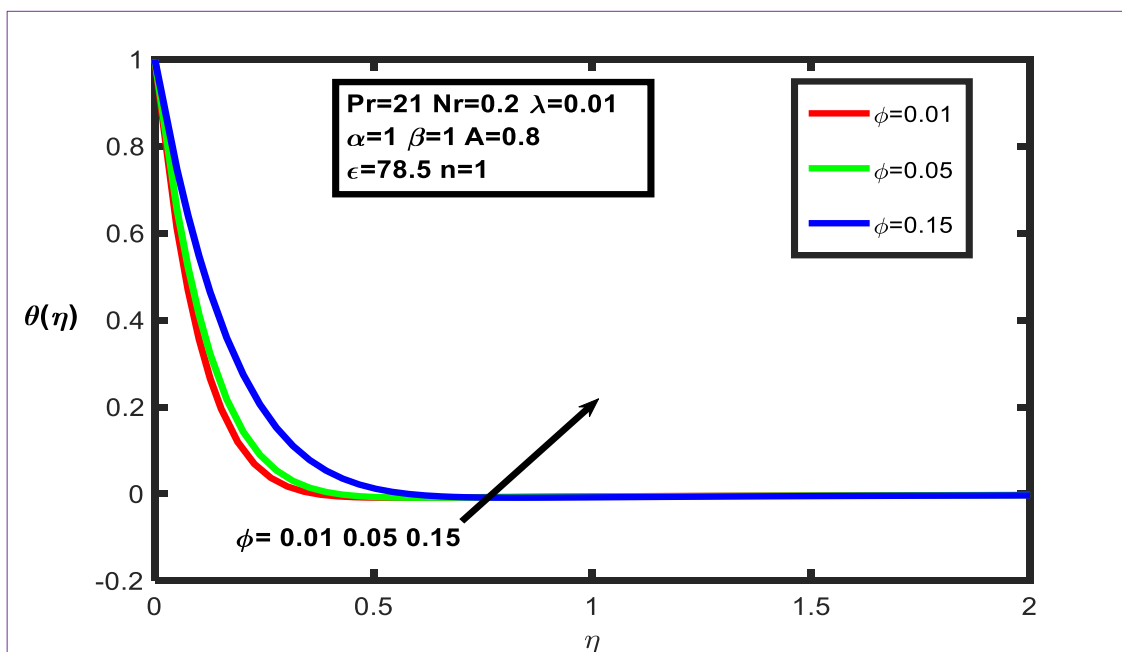


Figure 13: Effect of  $\phi$  on temperature profile  $\theta(\eta)$

Illustrations of the temperature profile with varying rates of Prandtl number ( $Pr$ ) are delineated in Figure 14. It is seen that the temperature profile increased with the enhancement of the Prandtl number. The Prandtl number transmits the fraction of the energy distribution to warm dispersion. As a consequence, the Prandtl number is the proportion of the kinematic consistency of the liquid to its conductance of radiation. This indicates that a greater Prandtl number ends in reduced warm conductivity and this is the explanation why growing Prandtl number attributes has the consequence of lessened heat flux stinginess.

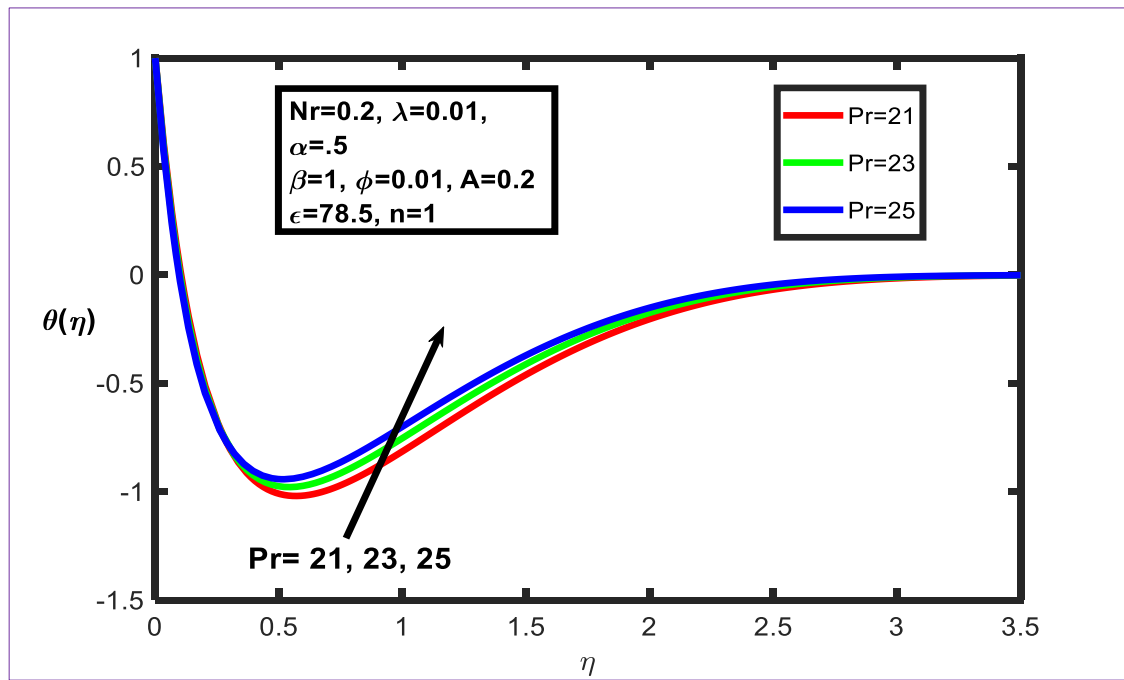


Figure 14: Effect of Pr on temperature profile  $\theta(\eta)$

For varied upsides of the adhesion boundaries (S), Figures 15 and 16 illustrate the speed profile and temperature profile. From the figures, it very well may be noticed that the speed profile and the temperature both abatement with growing up sides of the attraction boundary in the two scenarios for undiluted blood and copper undiluted blood.

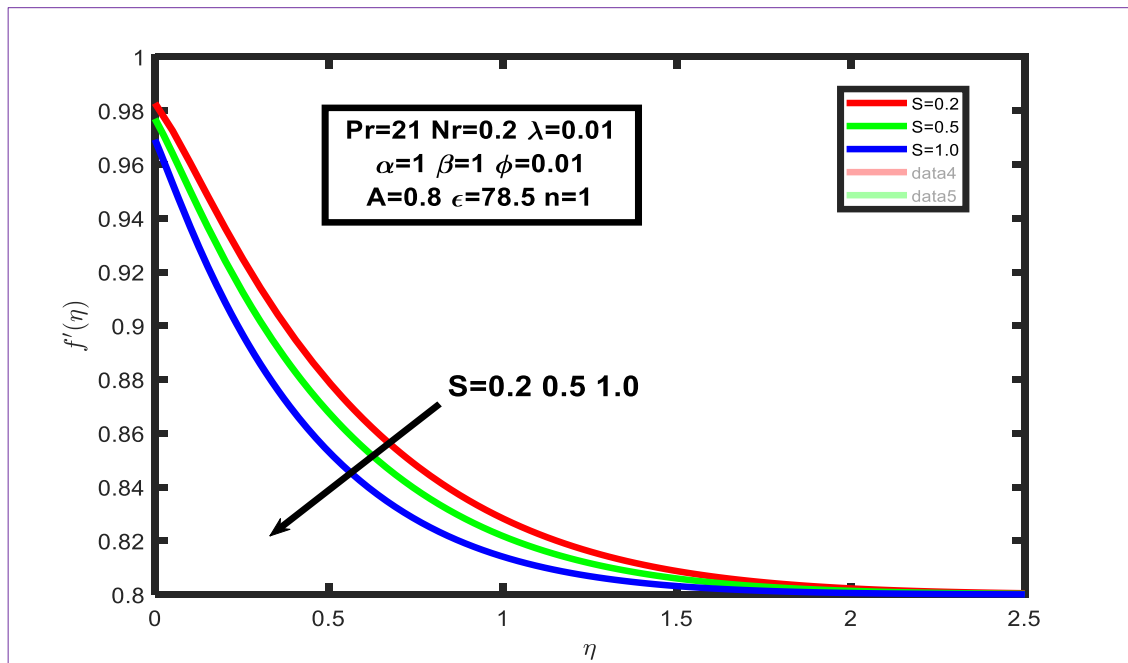


Figure 15: Effect of S on velocity profile  $f'(\eta)$

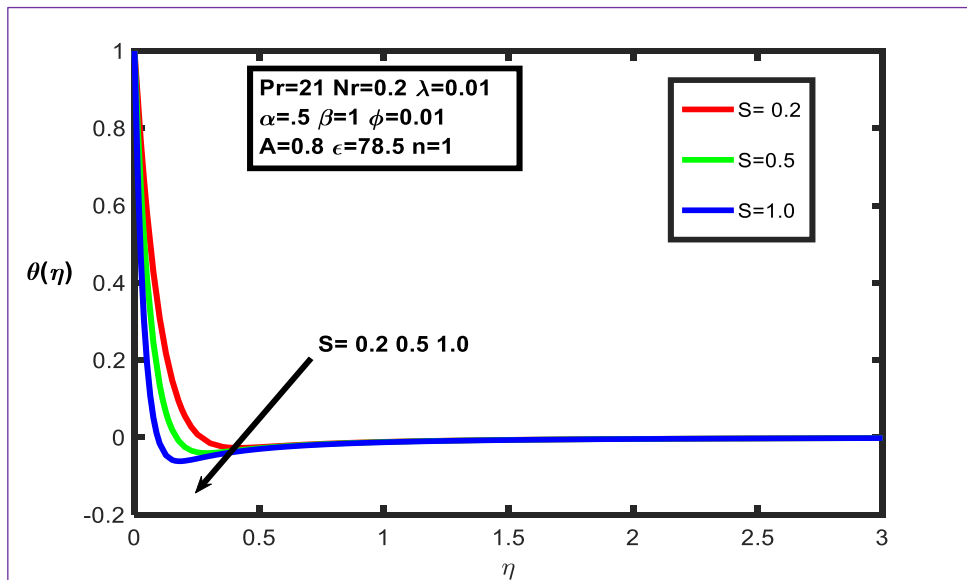


Figure 16: Effect of  $S$  on temperature profile  $\theta(\eta)$

Finally, the variations of physical quantities such as coefficient of skin friction  $f''(0)$  and local Nusselt number are graphically shown through Figures 17 and Figure 18 under several values of Prandtl number, radiation parameter, volume fraction and ratio parameter, respectively about the ferromagnetic number.

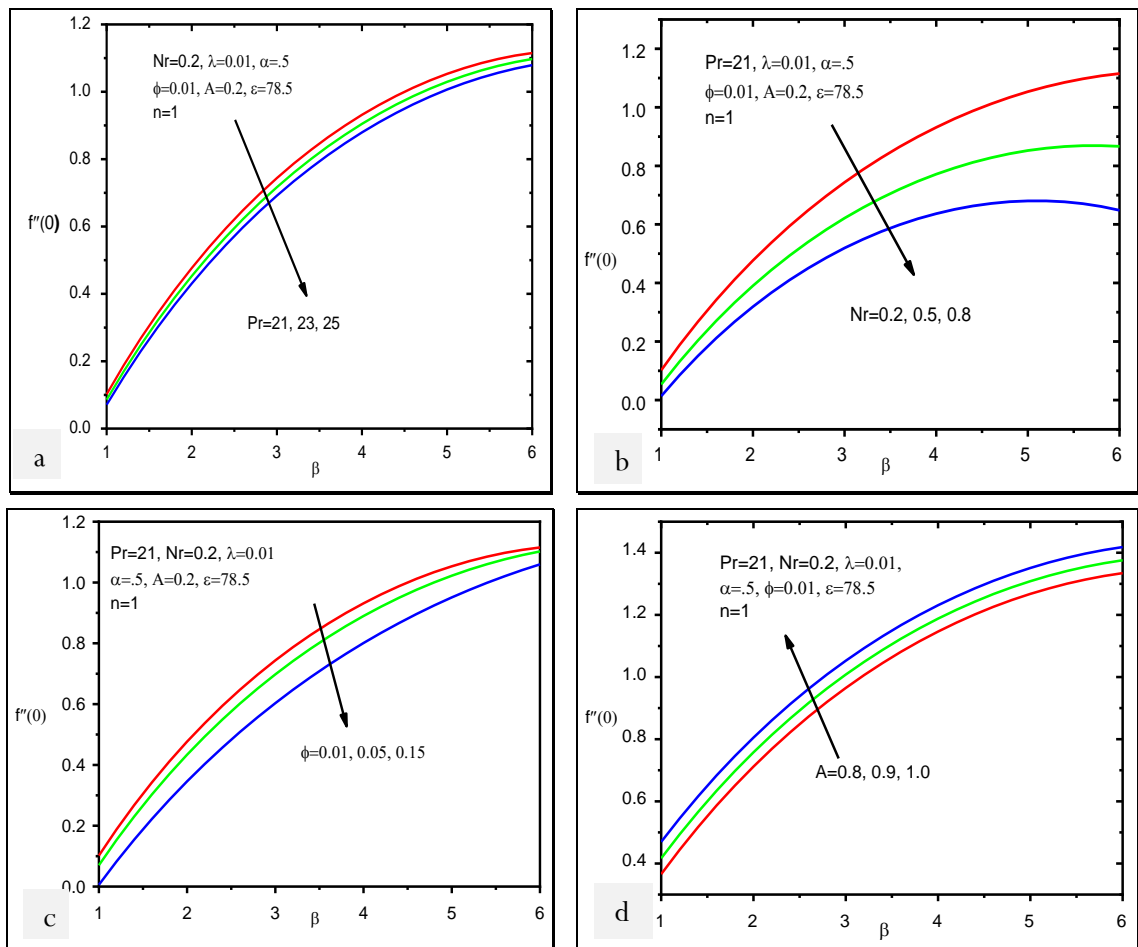


Figure 17: Skin friction co-efficient  $f''(0)$  with  $\beta$  for different values of (a)  $Pr$  (b)  $Nr$  (c)  $\phi$  (d)  $A$

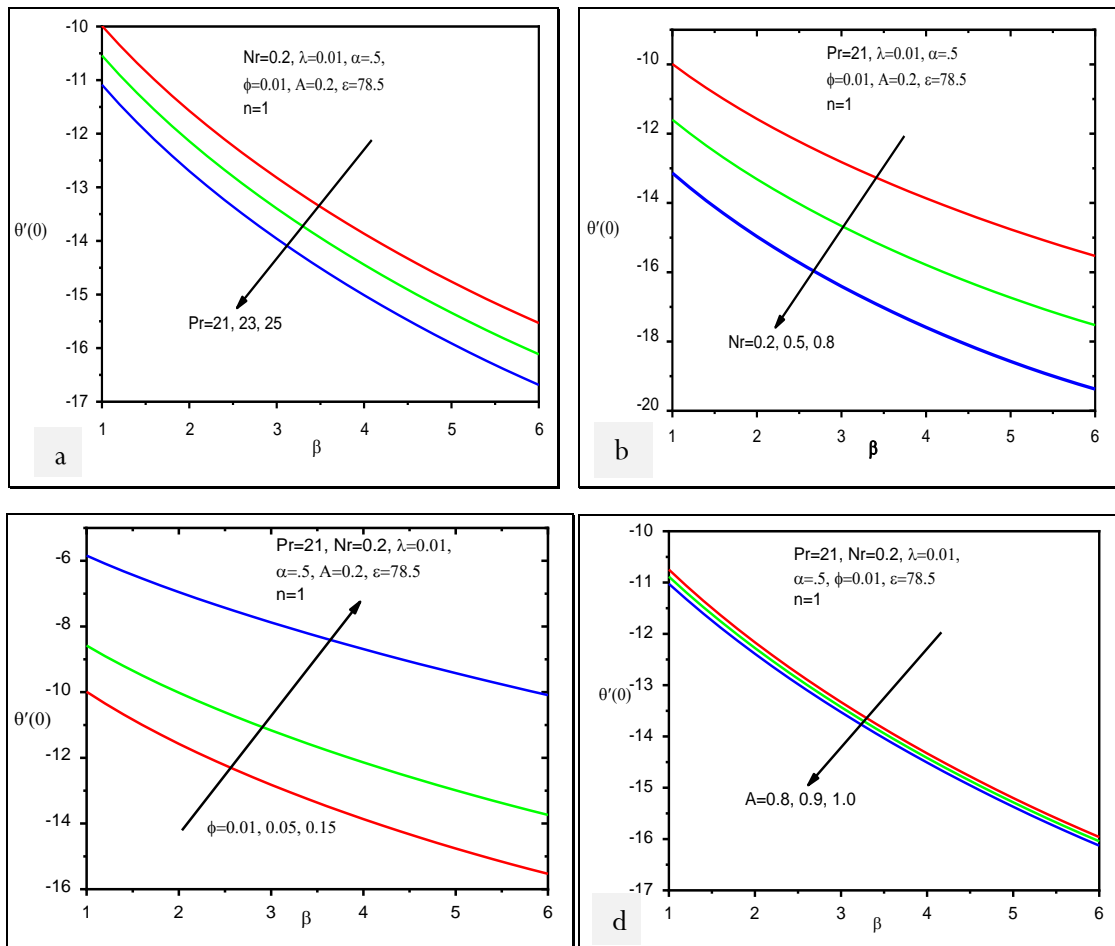


Figure 18: Local Nusselt Number  $\theta'(0)$  with  $\beta$  for different values of (a) Pr (b) Nr (c)  $\phi$  (d) A

It is seen that both  $f''(0)$  and  $\theta'(0)$  are reduced for enlarging values of radiation parameter and Prandtl number. For boosting values of particle volume fraction it is found that the rate of heat transfer accelerates but skin friction is reduced. In the case of the ratio parameter,  $f''(0)$  enhanced but reverse phenomena are found for  $\theta'(0)$ .

#### 4. Conclusion

A numerical investigation of blood-Cu has been conducted in this study in the presence of a magnetic dipole that passed through a stretching sheet. The governing PDEs are transformed into ODEs via suitable similarity variables and a well-known bvp4c technique is therefore applied to solve this problem computationally. Therefore, from the present numerical outcomes, we can summarize our findings as:

- (i) With enlarging values of the suction parameter, and radiation parameter both fluid velocity and temperature decline; whereas reverse phenomena are observed for the ratio parameter.
- (ii) Fluid velocity reduces for advancement values of dimensionless distance, first-order slip parameter, and volume fraction, while reverse results are found in temperature distributions case.
- (iii) For increment values of ferromagnetic number, fluid temperature decreases but velocity increases.

- (iv) Both skin friction and Nusselt number reduce for Prandtl number and radiation parameter.
- (v) For rising values of volume fraction, skin friction reduces but the rate of heat transfer increases.
- (vi) The rate of heat transfer of blood-Cu reduces for accelerating values of ratio parameter but increases in skin friction profile.

### Author contribution

M.G. Murtaza and Maria Akter: Carried out the formal analysis, investigation, conceptualization and drafted the manuscript. M. Ferdows: Carried out methodology, review, editing and supervision. All authors read and approved the final manuscript.

### Funding statement

This research did not receive any specific grant from funding agencies in the public, commercial, or not-for-profit sectors.

### Acknowledgements

We are grateful to Simulation Laboratory, Department of Mathematics, Comilla University for high configuration computer used in this work.

### Competing interest

The authors declare that they have no competing interests.

### References

- [1] S. Mansur, A. Ishak, and I. Pop, "Stagnation-point flow towards a stretching/shrinking sheet in a nanofluid using Buongiorno's model," *Proceedings of the Institution of Mechanical Engineers, Part E: Journal of Process Mechanical Engineering*, vol. 231, no. 2, pp. 172–180, Apr. 2017, <https://www.doi.org/10.1177/0954408915585047>
- [2] R. N. Jat and S. Chaudhari, "Magnetohydrodynamics boundary layer flow near the stagnation point of a stretching sheet," *Nuovo Cimento della Societa Italiana di Fisica B, General Physics, Relativity, Astronomy and Mathematical Physics and Methods*, vol. 123, no. 5, pp. 555–566, 2008, [Online]. Available: [http://inis.iaea.org/search/search.aspx?orig\\_q=RN:41058978](http://inis.iaea.org/search/search.aspx?orig_q=RN:41058978)
- [3] R. N. Jat, A. Neemawat, and D. Rajotia, "MHD boundary layer flow and heat transfer over a continuously moving flat plate," *International Journal of Statistika and Matematika*, vol. 3, no. 3, pp. 102–108, 2012. Available: [https://statperson.com/Journal/StatisticsAndMathematics/Article/Volume3Issue3/IJSA\\_M\\_3\\_3\\_4.pdf](https://statperson.com/Journal/StatisticsAndMathematics/Article/Volume3Issue3/IJSA_M_3_3_4.pdf)
- [4] C. Y. Wang, "Stagnation flow towards a shrinking sheet," *Int J Non Linear Mech*, vol. 43, no. 5, pp. 377–382, Jun. 2008, <https://www.doi.org/10.1016/j.ijnonlinmec.2007.12.021>
- [5] F. Aman, A. Ishak, and I. Pop, "Magnetohydrodynamic stagnation-point flow towards a stretching/shrinking sheet with slip effects," *International Communications in Heat and Mass Transfer*, vol. 47, pp. 68–72, Oct. 2013, <https://www.doi.org/10.1016/j.icheatmasstransfer.2013.06.005>
- [6] L. J. Crane, "Flow past a stretching plate," *Zeitschrift für angewandte Mathematik und Physik ZAMP*, vol. 21, no. 4, pp. 645–647, Jul. 1970, <https://www.doi.org/10.1007/BF01587695>



- [7] M. Miklavčič and C. Wang, “Viscous flow due to a shrinking sheet,” *Q Appl Math*, vol. 64, no. 2, pp. 283–290, Apr. 2006, <https://www.doi.org/10.1090/S0033-569X-06-01002-5>
- [8] M. J. Alam, M. G. Murtaza, E. E. Tzirtzilakis, and M. Ferdows, “Effect of thermal radiation on biomagnetic fluid flow and heat transfer over an unsteady stretching sheet,” *Computer Assisted Methods in Engineering and Science*, vol. 28, no. 2, pp. 81–104, 2021, <https://www.doi.org/10.24423/comes.327>
- [9] T. R. Mahapatra and A. S. Gupta, “Stagnation-point flow towards a stretching surface,” *Can J Chem Eng*, vol. 81, no. 2, pp. 258–263, Apr. 2003, <https://www.doi.org/10.1002/cjce.5450810210>
- [10] T. R. Mahapatra and A. S. Gupta, “Heat transfer in stagnation-point flow towards a stretching sheet,” *Heat and Mass Transfer*, vol. 38, no. 6, pp. 517–521, Jun. 2002, <https://www.doi.org/10.1007/s002310100215>
- [11] K. Vajravelu, “Viscous flow over a nonlinearly stretching sheet,” *Appl Math Comput*, vol. 124, no. 3, pp. 281–288, Dec. 2001, [https://www.doi.org/10.1016/S0096-3003\(00\)00062-X](https://www.doi.org/10.1016/S0096-3003(00)00062-X)
- [12] N. Bachok and A. Ishak, “Similarity solutions for the stagnation-point flow and heat transfer over a nonlinearly stretching/shrinking sheet,” *Sains Malaysiana*, vol. 40, no. 11, pp. 1297–1300, 2011. Available: [https://www.ukm.my/jsm/pdf\\_files/SM-PDF-40-11-2011/14%20Norfifah.pdf](https://www.ukm.my/jsm/pdf_files/SM-PDF-40-11-2011/14%20Norfifah.pdf)
- [13] P. Rana and R. Bhargava, “Flow and heat transfer of a nanofluid over a nonlinearly stretching sheet: A numerical study,” *Commun Nonlinear Sci Numer Simul*, vol. 17, no. 1, pp. 212–226, Jan. 2012, <https://www.doi.org/10.1016/j.cnsns.2011.05.009>
- [14] M. H. Matin, M. R. H. Nobari, and P. Jahangiri, “Entropy analysis in mixed convection MHD flow of nanofluid over a non-linear stretching sheet,” *Journal of Thermal Science and Technology*, vol. 7, no. 1, pp. 104–119, 2012, <https://www.doi.org/10.1299/jtst.7.104>
- [15] R. Cortell, “MHD flow and mass transfer of an electrically conducting fluid of second grade in a porous medium over a stretching sheet with chemically reactive species,” *Chemical Engineering and Processing: Process Intensification*, vol. 46, no. 8, pp. 721–728, Aug. 2007, <https://www.doi.org/10.1016/j.cep.2006.09.008>
- [16] R. Cortell, “Viscous flow and heat transfer over a nonlinearly stretching sheet,” *Appl Math Comput*, vol. 184, no. 2, pp. 864–873, Jan. 2007, <https://www.doi.org/10.1016/j.amc.2006.06.077>
- [17] A. Raptis and C. Perdikis, “Viscous flow over a non-linearly stretching sheet in the presence of a chemical reaction and magnetic field,” *Int J Non Linear Mech*, vol. 41, no. 4, pp. 527–529, May 2006, <https://www.doi.org/10.1016/j.ijnonlinmec.2005.12.003>
- [18] W. Shyy and R. Narayanan, “Fluid Dynamics at Interfaces,” 2010. [Online]. Available: <https://api.semanticscholar.org/CorpusID:126731947>
- [19] J. Alam, M. G. Murtaza, E. E. Tzirtzilakis, and M. Ferdows, “Application of biomagnetic fluid dynamics modeling for simulation of flow with magnetic particles and variable fluid properties over a stretching cylinder,” *Math Comput Simul*, vol. 199, pp. 438–462, Sep. 2022, <https://www.doi.org/10.1016/j.matcom.2022.04.008>
- [20] R. Cortell, “Effects of viscous dissipation and radiation on the thermal boundary layer over a nonlinearly stretching sheet,” *Phys Lett A*, vol. 372, no. 5, pp. 631–636, Jan. 2008, <https://www.doi.org/10.1016/j.physleta.2007.08.005>
- [21] S. Awang Kechil and I. Hashim, “Series solution of flow over nonlinearly stretching sheet with chemical reaction and magnetic field,” *Phys Lett A*, vol. 372, no. 13, pp. 2258–2263, Mar. 2008, <https://www.doi.org/10.1016/j.physleta.2007.11.027>
- [22] X. Huang and M. A. El-Sayed, “Gold nanoparticles: Optical properties and implementations in cancer diagnosis and photothermal therapy,” *J Adv Res*, vol. 1, no. 1, pp. 13–28, Jan. 2010, <https://www.doi.org/10.1016/j.jare.2010.02.002>

- [23] S. U. S. Choi and J. A. Eastman, "Enhancing thermal conductivity of fluids with nanoparticles," United States, 1995. [Online]. Available: <https://www.osti.gov/biblio/196525>
- [24] M. Ferdows, M. G. Murtaza, E. E. Tzirtzilakis, and F. Alzahrani, "Numerical study of blood flow and heat transfer through stretching cylinder in the presence of a magnetic dipole," *ZAMM - Journal of Applied Mathematics and Mechanics / Zeitschrift für Angewandte Mathematik und Mechanik*, vol. 100, no. 7, Jul. 2020, <https://www.doi.org/10.1002/zamm.201900278>
- [25] M. Ferdows, J. Alam, G. Murtaza, E. E. Tzirtzilakis, and S. Sun, "Biomagnetic flow with  $\text{CoFe}_2\text{O}_4$  magnetic particles through an unsteady stretching/shrinking cylinder," *Magnetochemistry*, vol. 8, no. 3, p. 27, Feb. 2022, <https://www.doi.org/10.3390/magnetochemistry8030027>
- [26] J. Alam, M.G. Murtaza, E.E. Tzirtzilakis, and M. Ferdows, "Mixed convection flow and heat transfer of Biomagnetic fluid with magnetic/non-magnetic particles due to a stretched cylinder in the presence of a magnetic dipole," *Proceedings of International Exchange and Innovation Conference on Engineering & Sciences (IEICES)*, vol. 8, pp. 76–83, Oct. 2022, <https://www.doi.org/10.5109/5909065>
- [27] T. Hayat, Z. Hussain, A. Alsaedi, and S. Asghar, "Carbon nanotubes effects in the stagnation point flow towards a nonlinear stretching sheet with variable thickness," *Advanced Powder Technology*, vol. 27, no. 4, pp. 1677–1688, Jul. 2016, <https://www.doi.org/10.1016/j.appt.2016.06.001>
- [28] S. R. R. Reddy and P. B. Anki Reddy, "Bio-mathematical analysis for the stagnation point flow over a non-linear stretching surface with the second order velocity slip and titanium alloy nanoparticle," *Frontiers in Heat and Mass Transfer*, vol. 10, Mar. 2018, <https://www.doi.org/10.5098/hmt.10.13>
- [29] E. E. Tzirtzilakis, "A mathematical model for blood flow in magnetic field," *Physics of Fluids*, vol. 17, no. 7, Jul. 2005, <https://www.doi.org/10.1063/1.1978807>
- [30] S. Mukhopadhyay, "MHD boundary layer flow and heat transfer over an exponentially stretching sheet embedded in a thermally stratified medium," *Alexandria Engineering Journal*, vol. 52, no. 3, pp. 259–265, Sep. 2013, <https://www.doi.org/10.1016/j.aej.2013.02.003>
- [31] J. Alam, M. G. Murtaza, E. Tzirtzilakis, and M. Ferdows, "Magnetohydrodynamic and ferrohydrodynamic interactions on the biomagnetic flow and heat transfer containing magnetic particles along a stretched cylinder," *European Journal of Computational Mechanics*, Feb. 2022, <https://www.doi.org/10.13052/ejcm2642-2085.3111>
- [32] K. Das, "Cu-water nanofluid flow and heat transfer over a shrinking sheet," *Journal of Mechanical Science and Technology*, vol. 28, no. 12, pp. 5089–5094, Dec. 2014, <https://www.doi.org/10.1007/s12206-014-1130-2>
- [33] M. G. Murtaza, E. E. Tzirtzilakis, and M. Ferdows, "Effect of electrical conductivity and magnetization on the biomagnetic fluid flow over a stretching sheet," *Zeitschrift für angewandte Mathematik und Physik*, vol. 68, no. 4, p. 93, Aug. 2017, <https://www.doi.org/10.1007/s00033-017-0839-z>
- [34] J. Alam, G. Murtaza, E. Tzirtzilakis, and M. Ferdows, "Biomagnetic fluid flow and heat transfer study of blood with gold nanoparticles over a stretching sheet in the presence of magnetic dipole," *Fluids*, vol. 6, no. 3, p. 113, Mar. 2021, <https://www.doi.org/10.3390/fluids6030113>

## NOMENCLATURE

|                   |   |
|-------------------|---|
| $U, V$            | Components of velocity                    |
| $U_e$             | Free stream velocity                      |
| $\mu$             | viscosity under dynamic conditions        |
| $\mu_{nf}$        | Effective friction coefficient            |
| $\rho_{nf}$       | Effective density of the nanofluid        |
| $T$               | Nanofluid temperature                     |
| $(\rho C_p)_{nf}$ | Thermal capacity of the base fluid        |
| $\phi$            | Volume fraction of nanoparticles          |
| $k_{nf}$          | Nanofluid's thermodynamic resistance      |
| $\mu_f$           | Viscosity under dynamic condition         |
| $\rho_f, \rho_s$  | Densities of fluid and solid              |
| $k_f, k_s$        | Thermal conductivities of fluid and solid |
| $H$               | Slope amplitude                           |
| $M$               | Magnetization                             |
| $K$               | Pyro-magnetic co-efficient                |
| $S$               | Suction/injection parameter               |
| $Pr$              | Prandtl number                            |
| $\lambda$         | Viscous dissipation parameter             |
| $\varepsilon$     | Dimensionless Curie temperature           |
| $\alpha$          | Dimensionless distance                    |
| $Nr$              | Radiation Conduction Parameter            |
| $\beta$           | Ferromagnetic parameter                   |
| $C_f$             | Skin friction coefficient                 |
| $Nu$              | Local Nusselt Number                      |
| $\tau_w =$        | Surface shearing stress                   |
| $q_w$             | Convective heat                           |